Bandwidth Optimization of a Wideband Co-Co Antenna Array on a Thin Flexible Dielectric using HFSS®

Joseph D. Majkowski

Harris Communication Systems
Rochester NY, 14610, United States
Jmajkows@harris.com

Abstract ─ This paper presents several novel techniques for designing a compact Co-Co antenna array for optimal performance over a broad frequency range of one and half octaves. The antenna was modeled and tested on 6 mil Polyimide composite, a thin, flexible, substrate, in order to meet size requirements. A slotting technique was used to increase both the impedance and gain bandwidth of the antenna. The final design produced an omnidirectional antenna with peak gain greater than 1 dBi and S(1,1) less than -8 dB over a frequency range of 2.8*F1. In order to make a manufacture-able antenna, the microstrip transmission line width was increased for co-axial feeding of the antenna with a second slotting technique.

Index Terms ─ Co-Co antenna, flexible, slotting, transmission line.

I. INTRODUCTION

Wide bandwidth antennas with omnidirectional performance at the horizon (azimuth plane) have grown in demand greatly over the last few years. This demand comes as military radios grow in both their capabilities and usable frequency range. The end user no longer picks up the radio just to make simple voice communication, but may also be utilizing the radio as a way to communicate mission plans, send pictures or video, or even act as a node in a network. These new capabilities offer many advantages but require much higher frequency ranges than traditional voice communications. Thus, to prevent adding another antenna to the soldiers burden, as well as to seamlessly switch between these capabilities, a single, wideband, antenna solution is needed.

The typical antenna of choice in military communication is a vertical monopole or dipole antenna with half wavelength resonant structure and broadband matching [1], [2]. However, the peak theoretical gain, 2.15 dBi, which one can achieve with a dipole or monopole may not be enough to achieve the high speed or even distance required with some of the higher frequency data waveforms. Thus we look to the coaxial, collinear (Co-Co) antenna [3], [4] to enhance the gain. It is seen that the gain and omnidirectional nature of the Co-Co antenna is very good; however, the bandwidth is very narrow. Thus, in order to improve bandwidth and functionality of the Co-Co antenna, various techniques such as altering element gap [5], moving feed location [6], tilting the elements [7], and varying element shapes [8] have been tried. While these techniques succeed, they only manage to achieve 10% to 15% increases in BW [5-7]. Other omnidirectional dipole printed antenna designs have been proposed in recent years [9], [10]. However, while these designs produce omnidirectional patterns, high gain and can increase bandwidth, they are also incredibly large and do not fit the required footprint for this antenna. In order to shrink overall size, techniques such as slots [11], [12] and utilizing a 3-D structure [12] have been utilized in more recent works.

In this paper, a novel 2 element wideband collinear dipole array with slots is designed, fabricated, and measured. The slotting technique helps to induce 2 modes of operation in the antenna and enhance both the gain and impedance bandwidth of the antenna. This technique keeps the current and voltage in phase for both a dipole excitation at low frequency and a Co-Co excitation for enhanced gains at the upper frequencies. Details of the proposed antenna are described and experimental results are presented along with the numerical results.

II. CO-CO ANTENNA BACKGROUND

The Co-linear, Co-polar (Co-Co) antenna array has been being used for decades due to its ease of manufacturing, high gain, and omnidirectional pattern.

The Co-Co antenna can be thought of as a set of $\ell/2$ co-axial transmission lines. The outer conductor and the inner conductor will alternate every $\ell/2$ in order to setup discontinuities. Voltage maximums will occur at these discontinuities between elements which encourages the antenna to radiate at these points. Thus, the more discontinuities the higher the antenna gain, however more elements produce a diminishing return

Submitted On: July 25, 2016
Accepted On: February 4, 2017

and comes at the cost of bandwidth.

Co-Co antennas can also be built with flat transmission line with one shorting pin at each end of the antenna. A second variation can also be built utilizing just one shorting pin farthest from the feed point. The shorting pins are utilized in the design to allow for the currents to be setup in-phase as seen in Fig. 1. Once the currents are in phase it allows for the antenna to have an omnidirectional radiation characteristic. The shorting pin closest to driving point of the antenna is primarily utilized as a balun to help reduce surface currents at the feed point, allowing more energy to make it to the antenna. However, the use of this shorting pin location comes at the cost of making the antenna much harder to match from a broadband impedance standpoint.

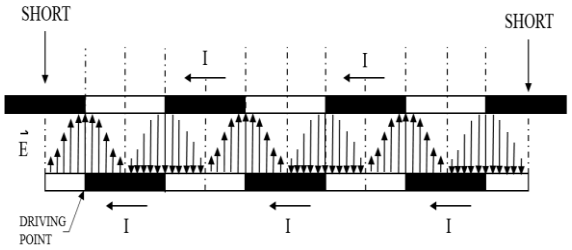

Fig. 1. Side view of the Co-Co antenna current and voltage distributions [8].

The shape of the elements can also be varied in order to achieve optimal performance. The tried element shapes have varied from circular, elliptical, rectangular and hybrids of any three of these shapes. It was found that by tapering the elements to form either circular or elliptical element shapes helps reduce side lobes levels. An image of these various techniques on 7 element Co-Co antennas can be seen below in Fig. 2. Image of the proposed antenna design are seen in Fig. 3. The slots on the top, bottom, and middle section are all controlled and defined in the same manner.

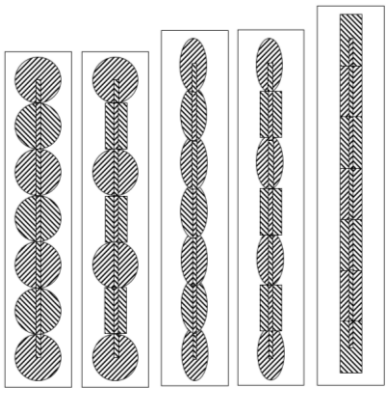

Fig. 2. Image of various element shapes and techniques of a 7 element design [8].

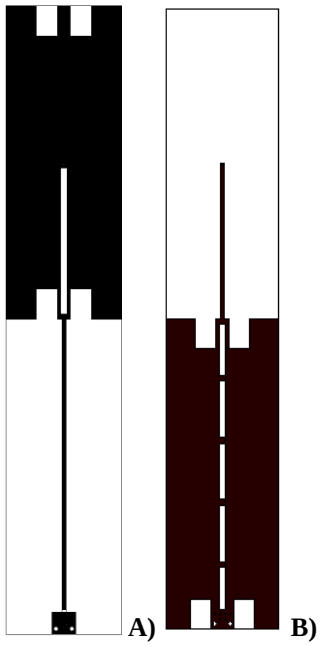

Fig. 3. Image of proposed antenna: (A) front view and (B) rear view.

III. SLOTTING TECHNIQUE

Given the advantages of the Co-Co antenna, it still did not have the bandwidth required. Thus, slots were added to increase the bandwidth.

Due to the nature of the Co-Co antenna array, the antenna elements need to be approximately $\ell/2$ in length, where ℓ is the center frequency's electrical length, in order to produce a maximum electric field at the reversal of ground plane and trace [13]. Due to required size of the antenna, the element lengths were chosen to be $\ell/2$ for a frequency slightly below $1.4*F_1$. However, it was seen that the S(1,1) of the antenna was only good for a bandwidth of approximately $1.8*F_1$ as seen in Fig. 3. This in turn caused the antenna to be a poor radiator at the higher frequencies ($2.8*F_1$). Four rectangular slots were cut into each element, two on the bottom and two on the top, in order to produce electrically shorter elements that extended the bandwidth. The slots were tuned using HFSS® parametric sweeps [14] to find the optimum length, width, and separation of the slots. The effect of the slots in both S(1,1) and electric field can be seen in Figs. 4 and 5. The S(1,1) improves significantly in the 1.7*F1-2.8*F1 range with the addition of the slots. The electric field shows that the antenna also radiates much more efficiently at 2.8*F1 with the addition of the slots.

The parametric sweeps of the slot parameters can be seen in Fig. 6. Slot length, (H-length), is swept 1 mm to 13 mm in the diagram. It is seen that as the length of the slot reached the 5 mm to 9 mm range that resonance circles start to form in the impedance and quickly

disappear in the swept frequency range above and below these lengths. In B, width of the slot, (H-width) is swept 1 mm to 6 mm. As this parameter increases, the impedance spirals clockwise and mimics the change presented by increasing a series inductor. Finally as the slot separation, (Hs), is swept from 2 to 8 mm, it is seen to have the effect of a decreasing parallel inductor. The closer the slots the better the impedance is and the farther apart the quicker the impedance begins to unravel.

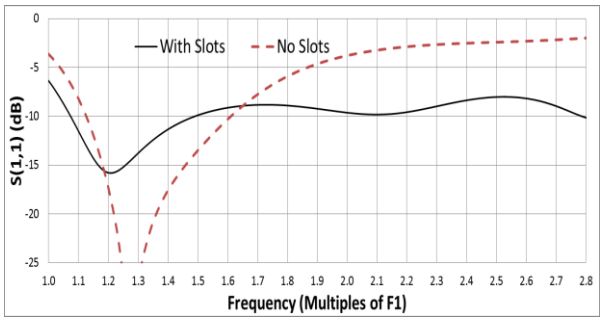

Fig. 4. S(1,1) in dB comparison of the slotted and non slotted antenna.

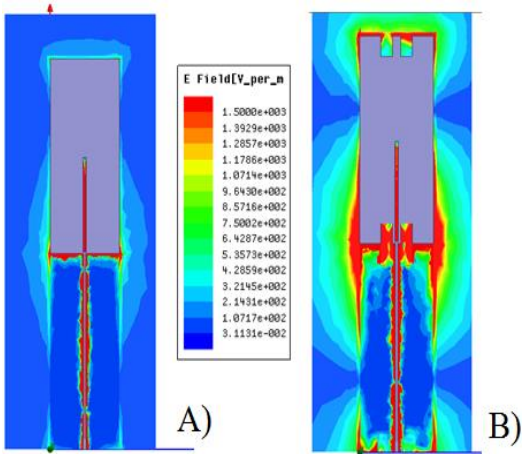

Fig. 5. Colored contour electric field plot (V/M) on a plane that bisects the PCB between the elements at 2.8*F_1. (A) No slots and (B) with slots.

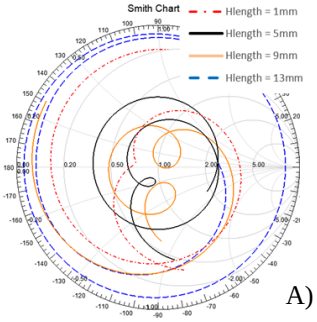

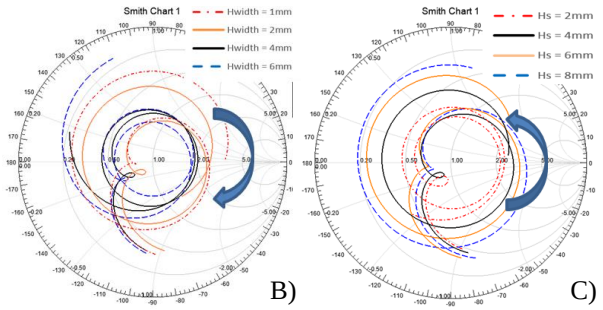

Fig. 6. Impedance of parametric sweep of: (A) H-length (length of slot), (B) H-width (width of slot), and (C) Hs (slot separation).

IV. MODES OF OPERATION

The antenna has two differing modes of operation. A "dipole" mode of operation, which occurs over the lowest frequencies (1-1.4)*F_1 and a "Co-Co" mode of operation that occurs over the rest of the frequency band (1.4-2.8)*F_1.

The "dipole" mode of operation performs as the name implies. The antenna begins to radiate, much like a dipole, at the element ends. This is due to the currents reaching a maximum at the junction between the two elements as seen in Fig. 7. The voltage thus reaches maximums at the end of the two elements which allows for the antenna to radiate as seen in Fig. 7. Here the performance is slightly lower than that of the "CoCo" mode as you are not able to radiate effectively at the junction between elements. The typical gain performance in this region of operation is 0-2 dBi at the horizon.

The "CoCo" mode of operation is when the antenna truly acts as an array. Currents are setup in this mode such that they reach maximums in the middle of each element which produces voltage maximums at the elements ends as well as the junction between the two elements. This can be seen in Fig. 8. Typical performance in this mode is more desirable as it surpasses the dipole mode with 1-4 dBi of gain at the horizon.

While it is certainly desirable to maintain the "CoCo" mode of radiation over the entire bandwidth it was simply not achievable. Both modes must be used to obtain and maximize bandwidth. The antenna was however able to be designed such that the crossover between the two modes caused no negative effects on the performance of the antenna. Thus, the antenna was able to cover the entire bandwidth with a slight 1 dB ripple in performance over some of the lower frequencies. The antenna is able to maintain an omnidirectional pattern throughout the transition between modes without introducing any side lobes to the pattern.

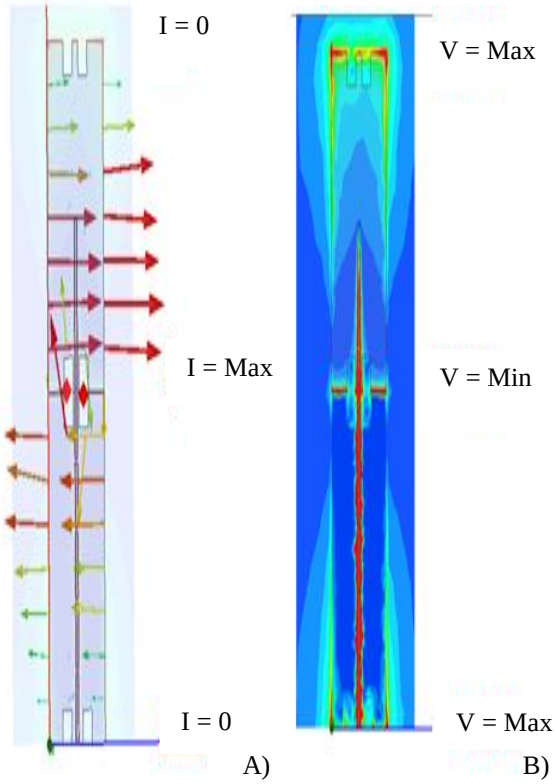

Fig. 7. HFSS simulation of the "dipole" mode of operation for: (A) current vectors at F_1 and (B) colored contour plot of electric field at F_1.

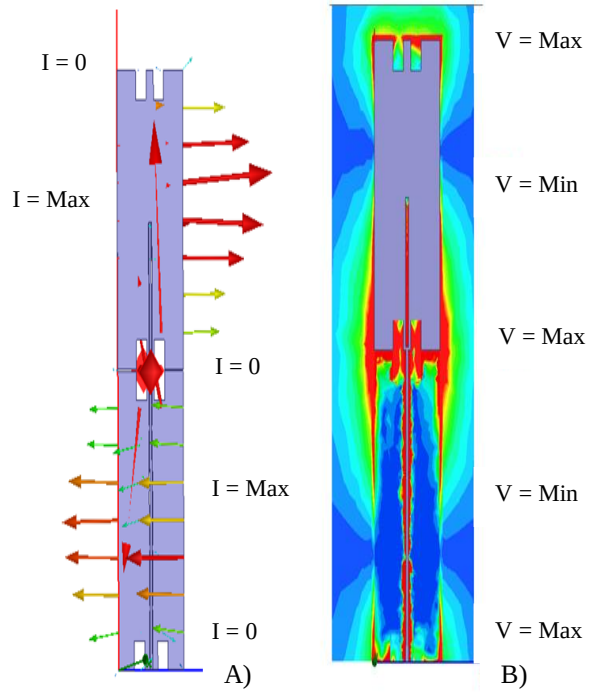

Fig. 8 HFSS simulation of the "CoCo" mode of operation for: (A) current vectors at $2*F_1$, and (B) colored contour plot of electric field between elements at $2*F_1$.

V. TRANSMISSION LINE ON A THIN SUBSTRATE

The transmission line width for a 50 ohm line on 6 mil polyimide is roughly 0.1 mm. This transmission line size is too thin and challenging to manufacture consistently. Also, due to the thin size of the transmission line there is concern from a manufacturing standpoint about the stability of the PCB when it is conformed to the inside of the radome. Thus, rectangular slots were cut in the ground plane, behind the transmission line to eliminate the overlap electric fields and leave only the fringe electric fields on the transmission line as seen in Fig. 9 [13]. The slots reduce the capacitance between the transmission line and the ground plane and allow flexibility to the designer in terms of the final width of the transmission line. That being said, the transmission line was designed to approximately 7 times its original width in order to allow for the board to be more consistently manufactured.

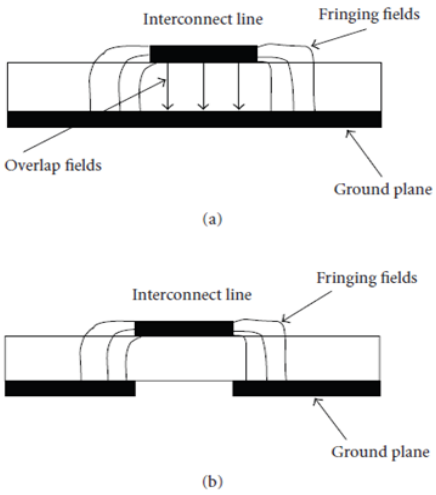

Fig. 9. Microstrip cross section for: (A) normal microstrip transmission line, and (B) slotted microstrip transmission line [13].

Shorting bars were also placed in the slot to connect both sides of the ground. The PCB image in Fig. 3 (B), rear view, shows the bottom element with this grid like setup of shorting bars. The bars were placed on the element to prevent voltage differential from giving rise to another mode forming on the antenna. The shorting bars were optimized in quantity, separation, location, and thickness. This was done with HFSS through parametric sweeps and genetic algorithms in order to arrive at their optimal performance.

VI. BENDING EFFECTS

In order to meet the required bandwidth, the PCB needed to be wider than the desired ¾ inch radome tube. In order to combat this problem the PCB was

designed on a flexible substrate to allow it to be curved and placed within the radome. Thus, the board was able to maintain the wider elements characteristics and still fit the mechanical envelope. The first step was designing the antenna on a flat PCB which drastically decreased the simulation time relative to a curved surface simulation. Thus, the runtime of optimizations and parametric sweeps was reduced and we were able to get the desired performance on a flat PCB much quicker.

The curved antenna can be simulated in HFSS with three approaches: use cylindrical geometry, use flat "sheet" geometry and wrap around a cylinder, then one can leave it as a sheet or "thicken" the sheet to better simulate the real world. Using cylindrical geometry, shapes can be cut out of a cylinder until the final antenna shape is realized. HFSS provides a simpler technique using "sheets", where one can create the geometry utilizing sheets [14]. Once the antenna geometry is created in two dimensions, it can be wrapped around a "non-model" cylinder. These "sheets" can be simulated by making the sheet a perfect E conductor with no thickness. This method will decrease run time at the cost of accuracy, but allows for many parametric runs to converge on the ideal solution. Once the design is optimized, one can "thicken" the "sheet" and assign it a metal material. The results shown are for a thickened sheet case.

It was noted that, as the PCB was transitioned from a flat to cylindrical shape inside a radome, that the impedance of the antenna took on more capacitance. The pattern at the horizon was also reduced slightly once the PCB was simulated in the cylindrical form. The maximum to minimum azmuthal pattern performance at $2*F_1$ was measured at approximately 4 dBi and increased as the frequency increased. Thus, the minimum specification for omnidirectionality was not met with its current dimensions.

It was found during simulations that the farther it wrapped around the radome, the worse the front-to-back ratio in the azmuthal pattern became. Thus, the element width needed to be decreased to a point that allowed for a good front to back ratio while maintaining the wide bandwidth and gain performance of the antenna. The antenna was then re-optimized with an element width that would provide good omnidirectional performance. The parameters that were re-optimized included the slots in terms of length, width, and separation, as well as the separation between the two elements. The antenna was thus successfully re-tuned to have good omnidirectional performance, within the radome, as seen in Fig. 10, while maintaining a good S(1,1) over the bandwidth.

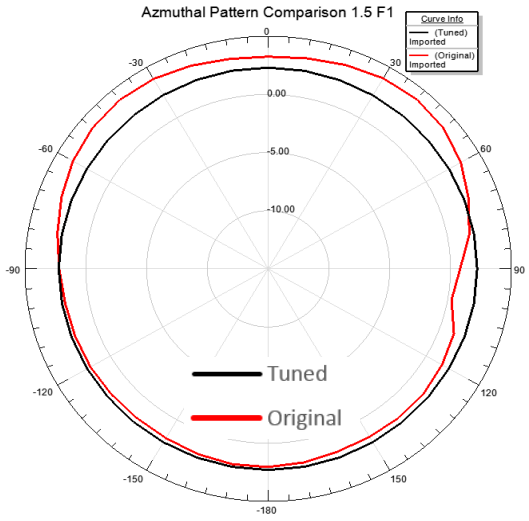

Fig. 10. Azmuthal pattern at $1.5*F_1$ of the antenna within the radome in its pre and post optimization form.

VII. DC BLOCK

The final antenna was then fabricated and placed within the radome. The antenna inside a clear radome is seen in Fig. 11, it shows the antenna does not conform to the inside of the radome. Rather, the rigidity of the PCB material keeps the board forming a slightly tighter C shape (view from top), than modeled. This discrepancy in bend radius of the board would explain difference in the model and proto-type performance.

The final designed antenna can be seen in Fig. 12. The board contains a break in the microstrip transmission line near the feed to incorporate a DC blocking capacitor. The capacitor was selected to be of a large enough value that it had absolutely no effect on the final antenna impedance. The location of the capacitor did however make a difference in the performance of the antenna. If placed too far up the transmission line the capacitor would shift the elevation of the pattern, reducing performance of the antenna at $\theta = 90°$ (horizon). Thus, on the first run of PCBS, a study was performed to determine the optimal location of the capacitor on the transmission line. This was done simply by removing the transmission line at various heights and soldering the capacitor in and comparing. It was found that the optimum location was as close as possible to the base of the board. However, the co-axial feeding forced the capacitor to be moved up slightly to allow for soldering of the co-axial line as well as some mechanical stability. A small, thin, flat portion of FR-4 was also added to the back of the board to provide mechanical stability to the capacitor as the PCB is bent and placed in the radome.

Fig. 11. Fabricated antenna board inside a clear tube.

Fig. 12. Image of both the front and back of the final fabricated PCB.

VIII. RESULTS

The S(1,1) of the antenna can be seen in Fig. 13. Overall the performance of the antenna matches closely with the simulation and the discrepancies can be chalked up to the antenna location in the radome and the excess bending the antenna is under. However, the -6 dB specification is met over the entire desired bandwidth. This specification is the maximum S(1,1) the radio can see before it is forced to cut-back power.

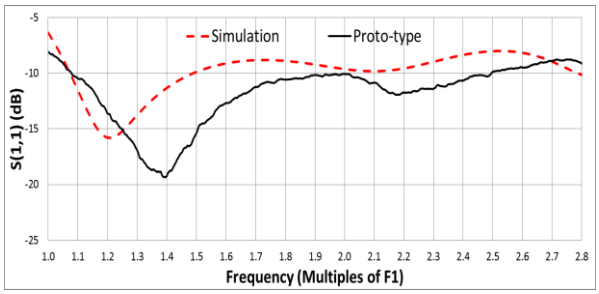

Fig. 13. S(1,1) in dB comparisons of the simulation and the fabricated antenna.

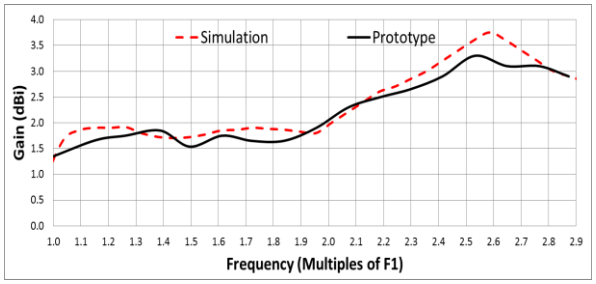

Fig. 14. Maximum gain comparisons at $\theta = 90$ of the simulation and the fabricated antenna.

The maximum gain of the antenna at $\theta = 90°$ is seen in Fig. 14. Overall, the two are very close in agreement. The elevation patterns of the antenna shown in Fig. 15 agree with the simulation and vary only slightly. It is seen that at F1 the pattern lobes down slightly while as we reach the end of the bandwidth of 2.8*F1 the pattern starts to lobe up slightly. However, despite the small discrepancies between the simulations and measurements, the patterns meet specification and show good performance at the horizon with no side lobes.

The antenna pattern was measured in the azimuthal plane at $\theta = 90°$ across the frequency band. This was done in order to verify the omnidirectional nature of the antenna. As seen in Fig. 16, the antenna ended up having a much higher maximum to minimum delta gain than the simulation. This was expected as the final shape of the antenna inside the radome varied slightly from the simulation. However, due to the nature of the original design, the fabricated antenna was still able to maintain a delta <3 dB over the frequency band.

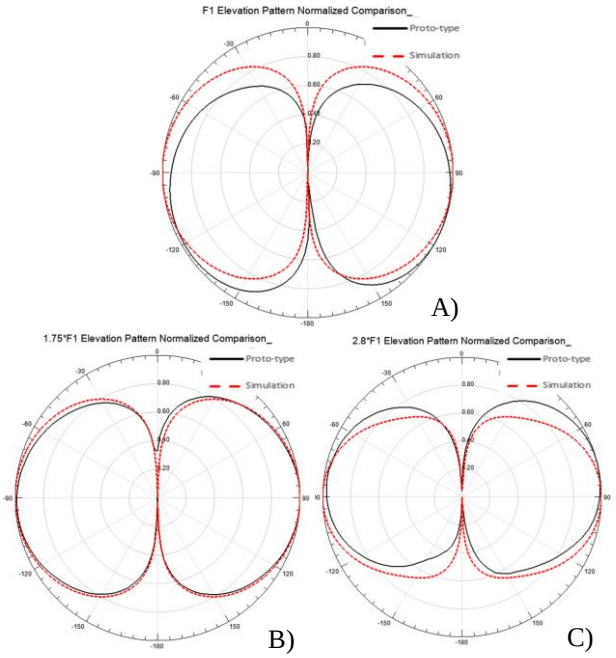

Fig. 15. Elevation pattern comparisons at: (A) F_1, (B) $1.75*F_1$, and (C) $2.8*F_1$.

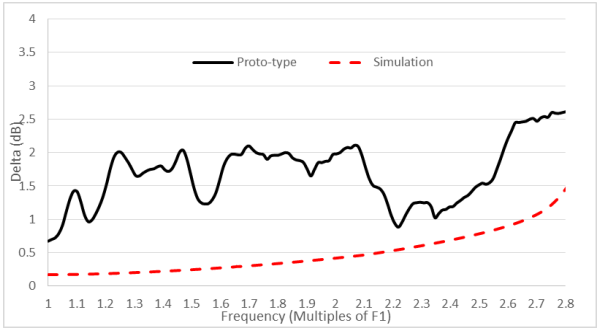

Fig. 16. Maximum to minimum delta gain comparison of azmuthal pattern at Θ=90.

IX. CONCLUSION

A very thin antenna was able to be designed and fabricated for performance over a very large bandwidth. Multiple modes of operation were required in order to meet the 1.5 octave bandwidth without a matching network. A slotting technique was able to be utilized to push the bandwidth limits of the "Co-Co" antenna further. A differing slotting technique was able to be utilized on a microstrip transmission line, on a thin dielectric, to increase the width of the transmission line of the antenna. This allowed for ease of manufacturing and for more consistency between antennas. The C-shape of the antenna produced undesirable capacitive loading as well as larger front-to-back ratios on the azmuthal patterns. The antenna needed to be re-optimized for its new shape. Overall, the measurements matched the simulations very well despite the differences between the simulation and the measurement configurations. All antenna specifications were able to be met over the 1.5 octave bandwidth.

It is also seen from the results that as the antenna is placed inside the radome the final shape will alter performance slightly. However, modeling these physical attributes of the system add to the simulation complexity and henceforth time. As computing and simulation tools become faster and more efficient these attributes of the system can also be simulated without adding cost to the design process. This will allow for the simulation and final product to be incredibly similar in their performance. Overall, despite these differences the antenna varied a small amount and still fell within the desired specifications.

ACKNOWLEDGEMENTS

The author would like to acknowledge Malcolm Packer of Harris Communications for his help in editing this paper and his constant guidance and support.

REFERENCES

[1] C. Sairam, et al., "Design and development of broadband blade monopole antenna," *2008 International Conference on Recent Advances in Microwave Theory and Applications*, 2008.

[2] Z. Zhang, et al., "Dual-band WLAN dipole antenna using an internal matching circuit," *IEEE Transactions on Antennas and Propagation*, vol. 53, no. 5, pp. 1813-1818, 2005.

[3] H. Wheeler, "A vertical antenna made of transposed sections of coaxial cable," *IRE International Convention Record*, vol. 4, pt. 1, pp. 160-164, 1956.

[4] T. J. Judasz and B. B. Balsley, "Improved theoretical and experimental models for the coaxial colinear antenna," *IEEE Transactions on Antennas and Propagation*, vol. 37, no. 3, pp. 289-296, 1989.

[5] L. Wang, et al., "A wideband omnidirectional planar microstrip antenna for WLAN applications," *2011 IEEE Electrical Design of Advanced Packaging and Systems Symposium (EDAPS)*, 2011.

[6] R. Bancroft and B. Bateman, "An omnidirectional planar microstrip antenna," *IEEE Transactions on Antennas and Propagation*, vol. 52, no. 11, pp. 3151-3153, 2004.

[7] Y. Zhou, et al., "A technique for improving bandwidth of COCO antenna array," *2008 4th International Conference on Wireless Communications, Networking and Mobile Computing*, 2008.

[8] R. Bancroft, *Microstrip and Printed Antenna Design*. 2nd ed, Raleigh, NC: SciTech, Print, 2009.

[9] K.-L. Wong, et al., "Omnidirectional planar dipole array antenna," *IEEE Transactions on Antennas and Propagation*, vol. 52, no. 2, pp. 624-628, 2004.

[10] Y. Yu, et al., "A wideband omnidirectional antenna array with low gain variation," *IEEE Antennas and Wireless Propagation Letters*, vol. 15, pp. 386-389, 2016.

[11] Y. Li, et al., "Design of penta-band omni-directional slot antenna with slender columnar structure," *IEEE Transactions on Antennas and Propagation*, vol. 62, no. 2, pp. 594-601, 2014.

[12] K. Wei, et al., "A triband shunt-fed omni-directional planar dipole array," *IEEE Antennas and Wireless Propagation Letters*, vol. 9, pp. 850-853, 2010.

[13] R. Sharma, et al., "Characteristic impedance of a microstrip-like interconnect line in presence of ground plane aperture," *International Journal of Microwave Science and Technology*, vol. 2007, ID 41951, 5 pages, 2007.

[14] ANSYS HFSS, 3D Full-wave Electromagnetic Field Simulation by Ansoft.

Joseph Daniel Majkowski received his B.S. and M.S. degrees in Electrical Engineering from the Rochester Institute of Technology in 2012.

He joined Harris Communications in 2012 where he began as a Systems Engineer. In 2013 he changed roles within the company to an RF and Antenna Design Engineer position.